communications biology

A Nature Portfolio journal

Article

https://doi.org/10.1038/s42003-025-07734-4

Characterization of *cis*-polyisoprene produced in *Periploca sepium*, a novel promising alternative source of natural rubber

Jingjiao Yong[1,2,3,4], Guodong Lu[1,2,4], Yingrui An[1,2], Sirui Lang[1,2], Hong Zhang[1,2] & Ren Chen[1,2] ✉

Natural rubber is an important industrial raw material and is almost exclusively produced from *Hevea brasiliensis* latex. Because *H. brasiliensis* is limited its cultivation to specific tropical regions, the insufficient capacity of natural rubber has become increasingly urgent. To develop a novel alternative plant for natural rubber production, we selected a perennial shrub *Periploca sepium*, which is widely distributed from tropical to temperate regions. *P. sepium* can produce latex and contains the rubber component polyisoprene with a high-molecular-weight distribution ranging from 10^4-10^6. Its main chain structure was identified as *cis*-1,4-polyisoprene, similar to that of *H. brasiliensis*. The polyisoprenes were observed to be present mainly in the secondary phloem adjacent to the cambium and pith, and almost entirely overlapped with the distributions of three rubber particle-associated proteins, *cis*-prenyltransferase (CPT), small rubber particle protein (SRPP) and rubber elongation factor (REF). The three genes were genome edited via CRISPR-Cas9 in *P. sepium*, and the total contents and high-molecular-mass regions of the *cis*-polyisoprenes in the transgenic plants with mutations were reduced to different degrees, indicating that the three genes apparently play important roles in natural rubber biosynthesis. This research will promote the development of *P. sepium* as an alternative source of natural rubber.

Natural rubber produced by plants, known as polyisoprene, consists of isoprene units $(C_5H_8)_n$ linked together in a 1,4 *cis*-configuration[1–4], which is the most widely used isoprenoid polymer. Natural rubber is considered one of the four most important and scarce industrial raw materials, along with steel, petroleum and coal, and its products have penetrated all aspects of industry and public life. Unlike most other biopolymers, natural rubber cannot be replaced by synthetic alternatives in many of its most significant applications due to its unique properties, which include resilience, elasticity, malleability, abrasion, impact resistance, and efficient heat dispersion[4–8]. In 2023, the Association of Natural Rubber Producing Countries (ANRPC, http://www.anrpc.org) reported that the global production of natural rubber was 14.89 million tons, but its consumption reached over 15.12 million tons, and demand is still steadily increasing. Although more than 2000 species of higher plants produce latex consisting of *cis*-polyisoprene[4,6,9–11], *Hevea brasiliensis* Muell. Arg (rubber tree) is currently the only commercial source of natural rubber because of its high rubber yield and the excellent physical properties of rubber products[4,11,12]. However, *H. brasiliensis* has strict climatic requirements, limiting its cultivation to specific tropical regions and preventing its expansion to nontropical countries[6,7,10]. Over 90% of natural rubber is produced in Southeast Asia, particularly in Malaysia, Thailand and Indonesia[6,13]. Consequently, the problem of insufficient capacity for natural rubber production has become increasingly urgent and has attracted worldwide attention.

In an effort to develop a novel alternative plant for commercial production of natural rubber in nontropical regions, no less than 8 botanical families, 300 genera and 2500 species that produce natural rubber in latex have been identified[6]. Only few species in addition to *H. brasiliensis* are known to produce rubber with relatively high molecular weights, i.e. *Parthenium argentatum* Gray and *Taraxacum kok-saghyz* Rodin, both of which are considered promising alternative rubber sources; other plants either

[1]Key Lab of Ministry of Education for Protection and Utilization of Special Biological Resources in Western China, Ningxia University, Yinchuan, Ningxia, 750021, China. [2]School of Life Science, Ningxia University, Yinchuan, Ningxia, 750021, China. [3]School of Pharmacy, Ningxia Medical University, Yinchuan, Ningxia, 750004, China. [4]These authors contributed equally: Jingjiao Yong, Guodong Lu. ✉e-mail: chenren@nxu.edu.cn

have not yet been studied in sufficient detail or produce rubber of inferior quality and low-molecular-weight, which are not adequate for the rubber industry[6,7,11,14–16]. However, *P. argentatum* and *T. kok-saghyz* have several disadvantages that become major barriers to their viable commercialization: the former does not tolerate the low winter temperatures in temperate-frigid regions and has been reported to trigger allelopathic influences on crops and livestock or cause severe human health problems[17,18], and the latter, which usually grows in cool and cold regions, mainly produces rubber in the roots, and unearthing roots is extremely labour intensive and may cause environmental problems[6,15,19–21].

In the present research, we selected 3 kinds of shrubs or herbs that produce latex, *Periploca sepium* Bunge, *Apocynum venetum* L. and *Cynanchum chinense* R.Br., for polyisoprene extraction and identification; these species are widely distributed in the arid and semiarid areas of Northwest, Northeast and North China. The molecular weight distributions of the extractives were analysed via gel permeation chromatography (GPC). Only *P. sepium*, which has a higher molecular weight distribution of polyisoprene, was considered promising as an alternative natural rubber source and was selected for further characterization. The molecular structure of its polyisoprene was determined by nuclear magnetic resonance (NMR), and the anatomical structures involved in the accumulation or biosynthesis of natural rubber were observed via Nile Red staining; in addition, three rubber particle-associated proteins, namely, *cis*-prenyltransferase (CPT), small rubber particle protein (SRPP) and rubber elongation factor (REF), were evaluated by immunostaining via spectral confocal laser scanning microscopy (SCLSM). The interactions between the three proteins were assayed via bimolecular fluorescence complementation (BiFC), and the comprehensive influences of the genes encoding the three proteins on rubber biosynthesis were evaluated in transgenic *P. sepium* via CRISPR-Cas9 genome editing. This research will promote the development of *P. sepium* as an alternative source for the production of natural rubber.

Results

Extractive identification from three kinds of plants that produce latex

Three kinds of plants (shrubs) that produce latex, *P. sepium*, *A. venetum* and *C. chinense* were selected for the rubber component polyisoprene extraction. The total contents of polyisoprene from the three plants were different by 1.12%, 0.51% and 0.21%, respectively ($p < 0.01$, Fig. 1a). The extracted polyisoprenes were subjected to GPC analysis for molecular weight distribution measurement. All of the polyisoprenes extracted from the three plants presented typical trimodal distribution curves. However, those of *A. venetum* and *C. chinense* were mainly centred at approximately 10^2–10^3, whereas that of *P. sepium* showed two peaks at approximately 10^2 and 10^3, and a distinct peak at approximately 10^5 (Fig. 1b). These results revealed that the polyisoprene extracted from *P. sepium* has a broader molecular weight distribution than those extracted from the other two plants do, especially in the 10^4-10^6 region.

According to the analysis of rubber in *H. brasiliensis*, polyisoprene usually has a bimodal distribution from 10^4-10^6[22], and the low-molecular-weight distribution less than 10^3 is considered polyprenols or dolichols (linear polyisoprene containing 9-23 isoprene units)[23–25]. It can be concluded that the extractives from *A. venetum* and *C. chinense* with low molecular weights or small molecular masses are mainly polyprenols, and only those with a high molecular weight distribution greater than 10^5 from *P. sepium* are suggested to be long-chain polyisoprene. The high molecular mass accounting for the peak area was 50.33%, and its number average molecular weight (*Mn*), weight average molecular weight (*Mw*) and molecular weight distribution index (*Mw*/*Mn*) were 4.24×10^4, 3.89×10^5 and 9.17, respectively (Fig. 1c, *P. sepium* peak 3).

Structural characterization of polyisoprene extracted from *P. sepium*

The polyisoprene extracted from *P. sepium* was analysed by ^{1}H-NMR and ^{13}C-NMR spectroscopy. Four major signals appeared at 2.04, 5.12, 2.05, and 1.68 ppm, which were assigned to the methylene (-CH_2-), methyne (-CH=), methylene (-CH_2-), and methyl (-CH_3) protons (H1, H3, H4, and H5) in the ^{1}H-NMR spectra, while five major signals appeared at 39.35, 135.18, 125.00, 26.37, and 23.40 ppm, which were assigned to the methylene (-CH_2-), olefinic (-Ċ=), methyne (=CH-), methylene (-CH_2-), and methyl (-CH_3) carbons (C1, C2, C3, C4, and C5) in the ^{13}C-NMR spectra, respectively (Fig. 2a). These signals were very similar to those of the *cis*-1,4-polyisoprene standard from *H. brasiliensis*, whereas they were different from those of the pure *trans*-1,4-polyisoprene standard from *Eucommia ulmoides*, particularly the characteristic signals at 1.98 and 16.01 ppm ascribed to the methyl (CH_3-) proton (H1) and methyl (-CH_3) carbon (C5) in the *trans*-isoprene units. This finding coincided with previous reports[24,26,27] and clearly indicated that the central isoprene units of the polyisoprene extracted from *P. sepium* are linked to each other head-to-tail in the *cis*-1,4-configuration.

Some minor signals were observed at 1.57, 1.58, 1.59, 1.60 ppm in the ^{1}H-NMR spectra and at 19.74, 15.95, 16.00, 16.13 ppm in the ^{13}C-NMR spectra (Fig. 2b), which were assigned to the methyl (-CH_3) protons or carbons (H5 or C5) in the ω-terminal (ω(*trans*)), *trans*-1 (ω-*trans*-*trans*), *trans*-2 (*trans*-*trans*-*trans*), and *trans*-3 (*trans*-*trans*-*cis*) isoprene units; these signals were distinctly different from the signals at 1.68 or 23.40 ppm in corresponding proton or carbon (H5 or C5) of the central isoprene units in the ^{1}H-NMR or ^{13}C-NMR spectra described above that were assigned to *cis*-configuration (Fig. 2a). These signals indicate that its ω-terminal isoprene units are followed by 2-3 isoprene units in the *trans*-1,4-configuration[26,28,29].

The signals at 4.57 and 62.28 ppm in the ^{1}H-NMR and ^{13}C-NMR spectra were assigned to the methylene (-CH_2-) proton or carbon (H4 or C4) in the α-terminal isoprene unit, and the signals at 3.64 and 45.36 ppm in the ^{1}H-NMR and ^{13}C-NMR spectra were assigned to the trimethyl (-$(CH_3)_3$) structure (Fig. 2a). These signals suggest that its α-terminal isoprene unit may consist of monophosphate and diphosphate (*cis*-α(*cis*)-$(OPO_3)_{1\text{-}2}$) linked with phospholipids ($N^+(CH_3)_3$)[30]. The results demonstrated that the main chain of the polyisoprene extracted from *P. sepium* is *cis*-1,4-polyisoprene composed of an ω-terminal *trans*-isoprene unit, 2-3 *trans*-isoprene units, *cis*-isoprene units, and an α-terminal *cis*-isoprene unit linked with phospholipids (Fig. 2a, Proposed structure of the main chain polyisoprene extracted from *P. sepium*).

In addition, four minor signals appeared at 4.73, 2.03, 1.26, and 1.60 ppm, which were assigned to the methylene (CH_2=), methyne (-ĊH-), methylene (-CH_2-), and methyl (-CH_3) protons (H1, H3, H4, and H5) in the ^{1}H-NMR spectra, and five minor signals appeared at 109.33, 150.52, 42.81, 29.34, and 19.74 ppm, which were assigned to the methylene (CH_2=), olefinic (=Ċ-), methyne (-ĊH-), methylene (-CH_2-), and methyl (-CH_3) carbons (C1, C2, C3, C4, and C5) in the ^{13}C-NMR spectra, respectively (Fig. 2c). These signals corresponded to the 3,4-isoprene unit, indicating that the polyisoprene extracted from *P. sepium* contains an abnormal 3,4-isoprene side group at approximately 3.6%, which was calculated from the signal area ratio between the methylene (CH_2=) proton (H1) in 3,4-isoprene and the methyne (=CH-) proton (H3) in *cis*-1,4-isoprene[31,32].

Anatomical observation of the structures involved in rubber accumulation in *P. sepium*

The relationships between the anatomical structures involved in the accumulation or biosynthesis of natural rubber and the particle-associated protein distributions in the stems of *P. sepium* were observed via SCLSM. The images in the cross-section under SCLSM bright field showed that *P. sepium* stem consisted distinct layers of cortex, phloem, cambium, xylem and pith (Fig. 3a–i). Some small circular holes similar to the laticifer structure were mainly distributed in the secondary phloem adjacent to the cambium and the pith layers, and the laticifer cells were surrounded by irregular parenchyma cells in the secondary phloem (Fig. 3a-ii) but were usually surrounded by 5-6 regular parenchyma cells in the pith (Fig. 3a-iii).

Since the cryosections were stained with Nile Red and Calcofluor White stain, according to the reference regions of interest (ROIs) selection and measurement, the cell wall, *cis*-polyisoprene and lipid body could be separated by their specific fluorescence wavelengths at maximum intensities

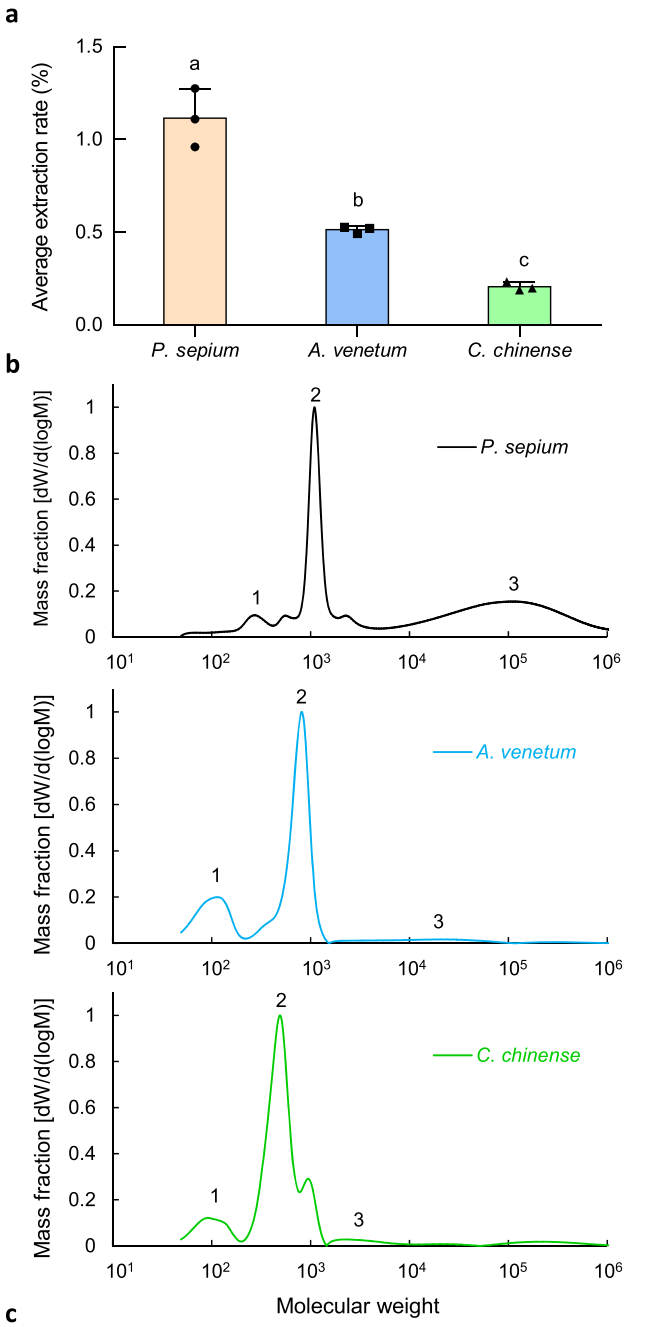

c

Plant	Peak	*Mn*	*Mw*	*Mw/Mn*	Area (%)
P. sepium	1	1.72×10^2	2.31×10^2	1.34	7.59
	2	1.09×10^3	1.32×10^3	1.21	42.08
	3	4.24×10^4	3.89×10^5	9.17	50.33
A. venetum	1	6.60×10^1	1.01×10^2	1.53	24.83
	2	7.29×10^2	1.35×10^3	1.85	72.51
	3	6.02×10^4	1.67×10^5	2.77	2.66
C. chinense	1	5.10×10^1	9.60×10^1	1.89	13.32
	2	5.31×10^2	1.22×10^3	2.30	84.40
	3	4.31×10^4	4.94×10^4	1.15	2.28

Fig. 1 | Total contents and molecular weight distributions of the polyisoprenes extracted from 3 plants. a The rubber component polyisoprenes were extracted from 3 plants that produce latex, *P. sepium*, *A. venetum* and *C. chinense*, and their total contents of polyisoprene were different by 1.12%, 0.51% and 0.21%, respectively; Data represent mean ± standard deviation, $n = 3$, and different letters indicate significant differences at $p < 0.01$. **b**, **c** The molecular weight distributions of the polyisoprenes extracted from the 3 plants were determined via GPC, and the number average molecular weight (*Mn*), weight average molecular weight (*Mw*), molecular weight distribution index (*Mw*/*Mn*) and each peak area of each sample was automatically calculated via the Eco-SEC Workstation provided by the GPC instrument. Compared with those of *A. venetum* and *C. chinense* that were mainly centred at approximately 10^2–10^3 (Peak 1, 2), *P. sepium* showed two peaks at approximately 10^2 and 10^3 (Peak 1, 2), and a distinct peak at approximately 10^5 (Peak 3, peak area was 50.33%, and its *Mw* was 3.89×10^5), indicating that the polyisoprene extracted from *P. sepium* has a broader molecular weight distribution, especially in the 10^4–10^6 region.

of 445 nm, 555 nm and 575 nm, which were unmixed in blue, yellow and magenta, respectively (Supplementary Fig. 1). In the cross-section, fluorescence images (yellow) revealed that the *cis*-polyisoprenes appeared mainly in the secondary phloem and the pith (Fig. 3b-i, ii, iii): most accumulated in the laticifer cells, and some dispersed in the surrounding cells. In the tangential section, fluorescence images (yellow) clearly showed that *cis*-polyisoprenes presented dispersed or nonarticulated linear shapes (Fig. 3b-iv, v, vi).

Immunostaining using primary antibodies against the three abundant rubber particle proteins PsCPT, PsSRPP and PsREF, which are considered playing important roles in natural rubber biosynthesis, were detected via SCLSM. The specificity of these antibodies against proteins extracted from *P. sepium* had been confirmed by Western blotting (Supplementary Fig. 2). The molecular weight of PsCPT (37.9 kDa) almost agreed with expectation, whereas those of PsSRPP and PsREF were higher than the calculated 26.6 kDa and 22.9 kDa, suggesting that they are post-translationally modified proteins[33]. Fluorescence images (magenta) of the cross-sections revealed that all of the three proteins appeared in the secondary phloem and the pith (Fig. 3c–i, iv, vii), almost entirely overlapping with the *cis*-polyisoprenes present. In the magnified images, the fluorescence distributions in the secondary phloem revealed that PsCPT and PsSRPP were more abundant than PsREF was (Fig. 3c-iii, vi, ix), especially PsSRPP, which even extended to some radial rays in the secondary xylem (Fig. 3c-vi), whereas all proteins were present sporadically in the pith (Fig. 3c-ii, v, viii).

BiFC assay of protein interactions between PsCPT, PsSRPP and PsREF

To further assay protein-protein interactions in living cells, *PsCPT*, *PsSRPP* and *PsREF* were cloned and constructed into the BiFC vectors pSPYNE and pSPYCE with a split YFP system, and were coinfiltrated into tobacco leaves via *Agrobacterium*-infiltrated transient expression, respectively. Upon coexpression of pSPYCE-PsCPT with pSPYNE-PsSRPP, pSPYCE-PsREF with pSPYNE-PsSRPP, or pSPYCE-PsCPT with pSPYNE-PsREF, strong YFP fluorescence signals were detected around the plasma membranes in the epidermal cell layers of the leaves (Fig. 3d), indicating that the protein-protein interactions occur between PsCPT with PsSRPP, PsSRPP with PsREF, and PsCPT with PsREF.

Influence evaluation of PsCPT, PsSRPP and PsREF on rubber biosynthesis in *P. sepium*

The comprehensive influences of the three genes encoding PsCPT, PsSRPP and PsREF on natural rubber biosynthesis were evaluated via CRISPR-Cas9 genome editing. Binary CRISPR-Cas9 vectors with three different sgRNA target sites for each gene (Fig. 4a) were introduced into the stem segments of *P. sepium* via *Agrobacterium*-mediated transformation. After infection, cocultivation, differentiation and selection, several plantlets are regenerated. PCR analysis confirmed that some plantlets produced the predicted CRISPR associated protein 9 (Cas9), synthetic green-fluorescent protein with S65T mutation (sGFP) and neomycin phosphotransferase (NPT) II DNA fragments, indicating that the transgenes were present in these transgenic plants.

Bidirectional sequencing of the genomic DNA isolated from the PCR+ plantlets indicated that a considerable portion of the plantlets exhibited mutations within or near the sgRNA target sites of the three genes, with

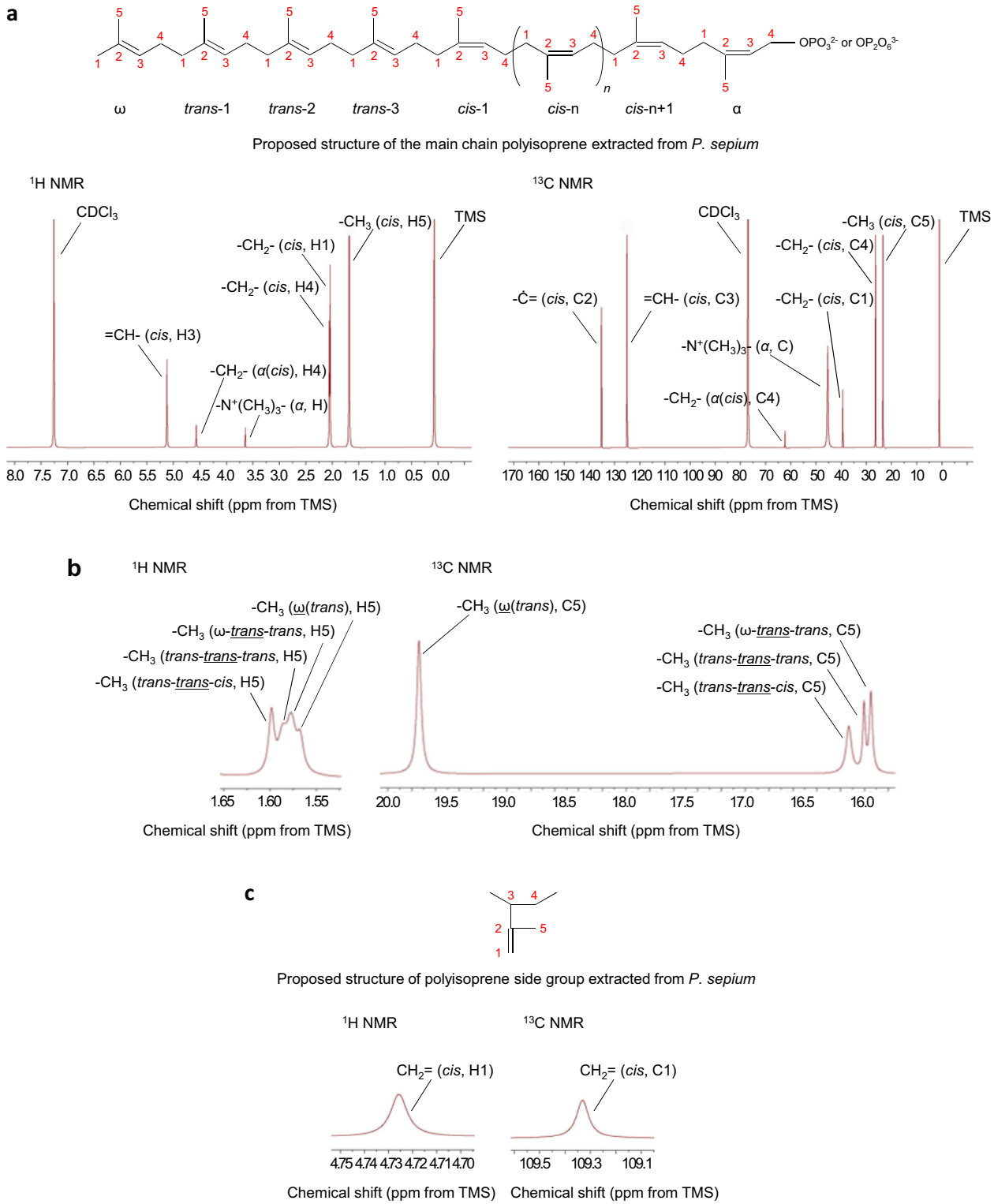

most deletions ranging from 1 to 37 nt, but rare substitutions or insertions (Supplementary Figs. 3–5).

The total contents of the *cis*-polyisoprenes extracted from the transgenic plants and their molecular weight distributions were determined via GPC analysis. Three representative mutagenesis plants of each *PsCPT*, *PsSRPP* and *PsREF* gene, namely, transgenic PsCPT-06, PsCPT-41, and PsCPT-63; PsSRPP-31, PsSRPP-34, and PsSRPP-36; and PsREF-17, PsREF-18, and PsREF-59, showed reduced total *cis*-polyisoprene contents to different degrees compared with that of the wild-type (nontransgenic negative, WT) control ($p < 0.01$), with the exception of PsCPT-63 (Fig. 4b). PsCPT-41 had a 37-nt deletion in the third sgRNA target site, resulting in the loss of 12 amino acid (aa) residues, along with 169 aa and termination codon alterations downstream, and the high-molecular-weight peak at approximately 10^4-10^6 was almost completely missing; in contrast, PsCPT-06, which had 2 nt substitutions in the second sgRNA target site and consequently only 2 aa alterations, exhibited the high-molecular-weight peak that was shifted forwards and smaller, and its area decreased from 46.35% in the WT to 5.96%; another PsCPT-63, which had 2 nt substitutions within

Fig. 2 | ^{1}H NMR and ^{13}C NMR spectra of the polyisoprene extracted from *P. sepium*. **a** Four major signals appeared at 2.04, 5.12, 2.05, and 1.68 ppm, which were assigned to the methylene (-CH_2-), methyne (-CH=), methylene (-CH_2-), and methyl (-CH_3) protons (H1, H3, H4, and H5) in the ^{1}H-NMR spectra, while five major signals appeared at 39.35, 135.18, 125.00, 26.37, and 23.40 ppm, which were assigned to the methylene, olefinic (-Ċ=), methyne, methylene, and methyl carbons (C1, C2, C3, C4, and C5) in the ^{13}C-NMR spectra, respectively, indicating that the central isoprene units of the polyisoprene are linked in the *cis*-1,4-configuration; The signals at 4.57 and 62.28 ppm in the ^{1}H-NMR and ^{13}C-NMR spectra were assigned to the methylene proton or carbon (H4 or C4) in the α-terminal isoprene unit, and the signals at 3.64 and 45.36 ppm in the ^{1}H-NMR and ^{13}C-NMR spectra were assigned to the trimethyl (-$(CH_3)_3$) structure; These signals suggest that the α-terminal isoprene unit of the polyisoprene may consist of monophosphate and diphosphate (*cis*-α(*cis*)-$(OPO_3)_{1\text{-}2}$) linked with phospholipids ($N^+(CH_3)_3$). **b** Four minor signals at 1.57, 1.58, 1.59, 1.60 ppm in the ^{1}H-NMR spectra and at 19.74, 15.95, 16.00, 16.13 ppm in the ^{13}C-NMR spectra, which were assigned to the methyl protons or carbons (H5 or C5) in the ω-terminal (ω(*trans*)), *trans*-1 (ω-*trans*-*trans*), *trans*-2 (*trans*-*trans*-*trans*), and *trans*-3 (*trans*-*trans*-*cis*) isoprene units; These signals were distinctly different from the signals at 1.68 or 23.40 ppm in corresponding proton or carbon (H5 or C5) of the central isoprene units in the ^{1}H-NMR or ^{13}C-NMR spectra that were assigned to *cis*-configuration, indicating that the ω-terminal isoprene units of the polyisoprene are followed by 2-3 isoprene units in the *trans*-1,4-configuration. **c** Four minor signals appeared at 4.73, 2.03, 1.26, and 1.60 ppm, which were assigned to the methylene, methyne, methylene, and methyl protons (H1, H3, H4, and H5) in the ^{1}H-NMR spectra, and five minor signals appeared at 109.33, 150.52, 42.81, 29.34, and 19.74 ppm, which were assigned to the methylene, olefinic, methyne, methylene, and methyl carbons (C1, C2, C3, C4, and C5) in the ^{13}C-NMR spectra, respectively. These signals corresponded to the 3,4-isoprene unit, indicating that the polyisoprene contains an abnormal 3,4-isoprene side group.

and near the first sgRNA target site and only 1 aa alteration, exhibited the high-molecular-weight peak that was shifted forwards and its area decreased to 14.55%. Similarly, in PsSRPP-31 or PsSRPP-36, which had 2- or 1-nt deletions in the first sgRNA target site, resulting in 159 or 154 aa and termination codon alterations downstream, respectively, the high-molecular-weight peak was completely absent, whereas PsSRPP-34, which had 7- and 2-nt deletions in the first and second sgRNA target sites, and 1-nt substitution near the second sgRNA target site, resulting in a loss of 3 aa and 19 aa alterations downstream, exhibited the high-molecular-weight peak that was shifted forwards and significantly reduced in area to 5.97%; PsREF-17, which had 2-, 5-, 27-nt deletions in the three sgRNA target sites, resulting in a loss of 11 aa and 130 aa and termination codon alterations downstream, exhibited no high-molecular-weight peak; PsREF-18, which had 2- and 1-nt deletions in the first and third sgRNA target sites and a 1-nt insertion in the second sgRNA target site, resulting in 140 aa and termination codon alterations downstream; and PsREF-59, which had 5- and 1-nt deletions in the first and third sgRNA target sites and a 1-nt substitution in the third sgRNA target site, resulting in a loss of 2 aa and 145 aa alterations downstream, both exhibited a forwards-shifted high-molecular-weight peak with a significantly reduced area, i.e. 5.81% or 7.43% (Fig. 4c, d). These results indicated that mutagenesis of these three genes, *PsCPT*, *PsSRPP* and *PsREF*, can down-regulate the biosynthesis of *cis*-polyisoprenes in *P. sepium*.

Discussion

In recent decades, the demand for natural rubber has continued to increase, and further production of natural rubber from *H. brasiliensis* has been limited to simply planting more acreage and cultivating technical improvements, because of this species' strict growing conditions, susceptible to various infectious diseases, small genetic diversity, etc[6,10,21,34]. A shortage of natural rubber is expected in the near future. Although synthetic polyisoprene rubber has been successfully obtained using petroleum derivatives as starting materials under stereospecific catalysts and its application scopes continue to expand, unexpectedly, despite all the efforts, some properties (such as superior mechanical properties) of natural rubber are difficult to match even when both polymers have the same stereoregularity. This is because natural rubber is considered a naturally occurring nanocomposite. Its nanostructure and non-rubber components like proteins and lipids, even if the differences are very small, also influence rubber properties. That is to say, synthetic rubber alternatives are still unable to completely replace natural rubber in many significant applications[4–8]. Consequently, it is necessary to search for other species for natural rubber production to meet its ever-increasing demands[6,7,10,11,15,16]. In this study, we present a new alternative source, *P. sepium*, which can produce latex in its leaves, branches, stems, roots and contains the rubber component *cis*-polyisoprene at approximately 1.12% (*w*/*w*, the residue weight obtained from chloroform extraction/sample fresh weight), whose molecular weight distribution is broader than those of two other plants, *A. venetum* and *C. chinense*, especially in the 10^4–10^6 high-molecular-weight region, according to GPC analysis. Its high molecular mass accounting for the peak area was 50.33%, and its *Mw* was 3.89×10^5, which was slightly less than that of *H. brasiliensis* (*Mw* 5×10^5-1.31×10^6) and approaching or greater than those of other alternative species, *P. argentatum* (*Mw* 4.76×10^5–5.77×10^5), *T. kok-saghyz* (*Mw* 4×10^3–3×10^5) and *Asclepias speciosa* (*Mw* 5.2×10^4)[6,7,10,14,15,35]. Since an *Mw* of 10^5 or more is appropriate for commercial applications[14], *P. sepium* is regarded as having potential for development as an alternative source for natural rubber production.

The main chain of the polyisoprene extracted from *P. sepium* is *cis*-1,4-polyisoprene. It is composed of an ω-terminal *trans*-isoprene unit, 2-3 *trans*-isoprene units, *cis*-isoprene units, and an α-terminal *cis*-isoprene unit linked with phospholipids, as determined via ^{1}H-NMR and ^{13}C-NMR spectroscopy analysis. The molecular structure is in good accordance with that of *H. brasiliensis* or other *cis*-polyisoprene-producing plants, such as *Solidago altissima*[26,29,36,37]. It can be presumed that in the initiation phase, the primers (initiators) of *cis*-polyisoprene polymerization in *P. sepium* comprise 3 types of allylic diphosphates, namely geranyl diphosphate (GPP, 2 isoprene units), farnesyl diphosphate (FPP, 3 isoprene units) and geranylgeranyl diphosphate (GGPP, 4 isoprene units). All of these are in the *trans*-1,4-configuration and are condensed by isopentenyl diphosphate (IPP, 1 isoprene unit) and its isomer dimethylallyl diphosphate (DMAPP) through the *trans*-isoprenyl diphosphate synthases of GPP, FPP, GGPP. This is the reason why there are 2-3 *trans*-isoprene units on the ω-terminal. The chain is subsequently extended by adding thousands of IPP to the primers in the *cis*-1,4-configuration. This addition (condensation) is carried out through the *cis*-isoprenyl diphosphate synthase, which is also referred to as *cis*-prenyltransferase (CPT, EC 2.5.1.20) in the *cis*-polyisoprene producing plants. In the final phase, the α-terminal forms and its monophosphate or diphosphate linked with phospholipids by hydrogen bound, when the size of the rubber droplet reaches a point where it does not allow further polymerization[3,4,7,28,31]. In addition, the polyisoprene extracted from *P. sepium* also contains a 3,4-isoprene abnormal side group at approximately 3.6%. This percentage appears to be higher than that from *H. brasiliensis*, which is usually lower than 2%[28,31,32]. An abundance of side groups may increase the rubber viscosity and stability to oxygen and heat[38].

The *cis*-polyisoprenes in *P. sepium* stem cryosections were observed via Nile Red histochemical staining under SCLSM. Nile Red is an uncharged lipophilic dye with intense fluorescence, and *cis*- or *trans*-polyisoprenes can be successfully distinguished from lipid bodies because their fluorescence wavelengths differ by 20–30 nm[33,39,40]. The *cis*-polyisoprenes mainly appeared in the secondary phloem adjacent to the cambium and pith layers, and most of them accumulated in the laticifer cells in dispersed or non-articulated linear shapes, with some particles dispersed in the surrounding cells. These observations suggested that *cis*-polyisoprene biosynthesis in *P. sepium* may first start in immature laticiferous cells as granules and then accumulate and fuse in the inner space along with mature laticiferous cells to laticifers. Laticifers in high-latex production trees, such as *H. brasiliensis*, are often continuous, concentric layered articulated laticifers in the secondary phloem, whereas nonarticulated laticifers are distributed at the outermost laticifer layer in the bark. However, trees with low latex production, such as

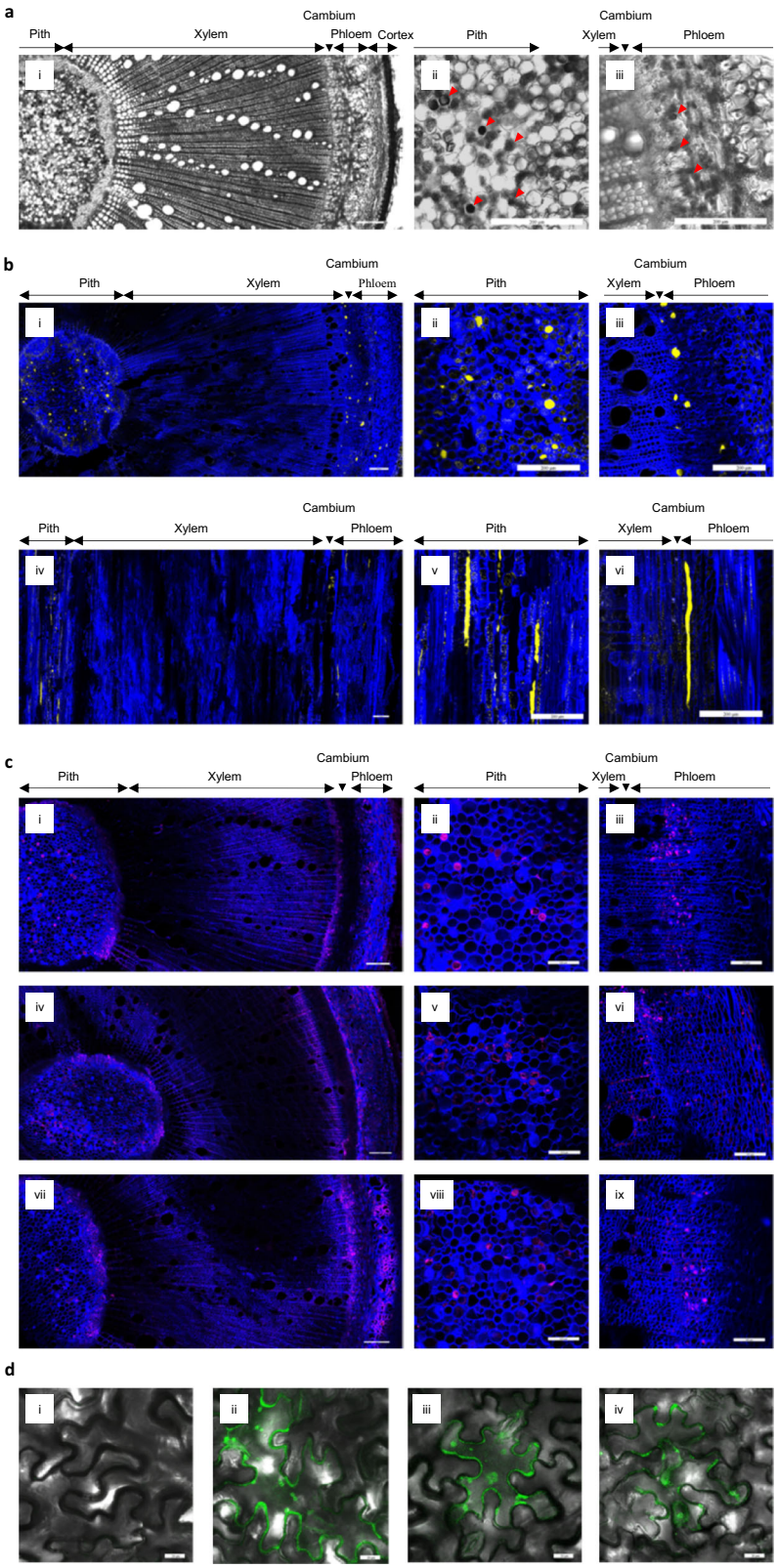

Fig. 3 | Natural rubber accumulation, rubber particle-associated protein distributions and interactions in *P. sepium*. **a** The images in the cross-section under SCLSM bright-field showed that *P. sepium* stem consisted distinct layers of cortex, phloem, cambium, xylem and pith (i); Some small circular holes similar to the laticifer structure were mainly distributed in the secondary phloem adjacent to the cambium and the pith layers, and the laticifer cells were surrounded by irregular parenchyma cells in the secondary phloem (ii), but were usually surrounded by 5-6 regular parenchyma cells in the pith (iii); Red arrow, laticifers; Scale bars, 200 μm. **b** The cryosections were stained with Nile Red and Calcofluor White stain for the detection of *cis*-polyisoprene and the cell wall under SCLSM; Fluorescence images (yellow) in the cross-section revealed that *cis*-polyisoprenes appeared mainly in the secondary phloem and the pith (i); Most accumulated in the laticifer cells, and some dispersed in the surrounding cells (ii, iii); Fluorescence images in the tangential-section showed that *cis*-polyisoprenes presented disperse or nonarticulated linear shapes (iv, v, vi); Yellow, *cis*-polyisoprene; Blue, cell walls; Scale bars, 200 μm. **c** Immunostaining using primary antibodies against the rubber particle-associated proteins PsCPT, PsSRPP and PsREF, were stained with Alexa Fluor 555 and Calcofluor White stain for the detection of the secondary antibody Donkey Anti-Rabbit IgG and the cell wall via SCLSM; Fluorescence images (magenta) of the cross-sections revealed that all of the three proteins appeared in the secondary phloem and pith (i, iv, vii; Scale bars, 200 μm), almost entirely overlapping with the *cis*-polyisoprenes present; The fluorescence distributions in the secondary phloem revealed that PsCPT and PsSRPP were more abundant than PsREF was (iii, vi, ix; Scale bars, 100 μm), especially PsSRPP, which even extended to some radial rays in the secondary xylem (vi), whereas all proteins were present sporadically in the pith (ii, v, viii; Scale bars, 100 μm); Magenta, *cis*-polyisoprene; Blue, cell walls. **d** Protein interactions of PsCPT, PsSRPP and PsREF determined via BiFC in tobacco leaves; Compared with that of empty pSPYNE and pSPYCE coinfiltration (negative control) (i), YFP fluorescence signals (green) in coexpression of pSPYCE-PsCPT with pSPYNE-PsSRPP, pSPYCE-PsREF with pSPYNE-PsSRPP, or pSPYCE-PsCPT with pSPYNE-PsREF, were detected around the plasma membranes in the epidermal cell layers, indicating that the protein-protein interactions occur between PsCPT with PsSRPP (ii), PsSRPP with PsREF (iii), and PsCPT with PsREF (iv); Scale bars, 20 μm.

P. argentatum, lack latex-producing cells[41] but instead produce resin in resin canals, which are predominantly present in parenchyma tissue, and in the pith, and many are not continuous[33]. *P. sepium* is likely in between, developing laticiferous cells or laticifers in the secondary phloem and pith but in a nonarticulated structure.

The fluorescence images of immunostaining under SCLSM revealed that the *cis*-polyisoprenes presented almost entirely overlapping with three proteins involved in rubber synthesis, PsCPT, PsSRPP and PsREF, and all of them appeared in the secondary phloem and the pith. PsCPT and PsSRPP were more abundant than PsREF in the secondary phloem, especially PsSRPP, which even extended to some radial rays in the secondary xylem, whereas all proteins were sporadically present in the pith. These results demonstrated that the biosynthesis of *cis*-polyisoprenes (natural rubber) mainly takes place in the laticiferous cells within the secondary phloem and

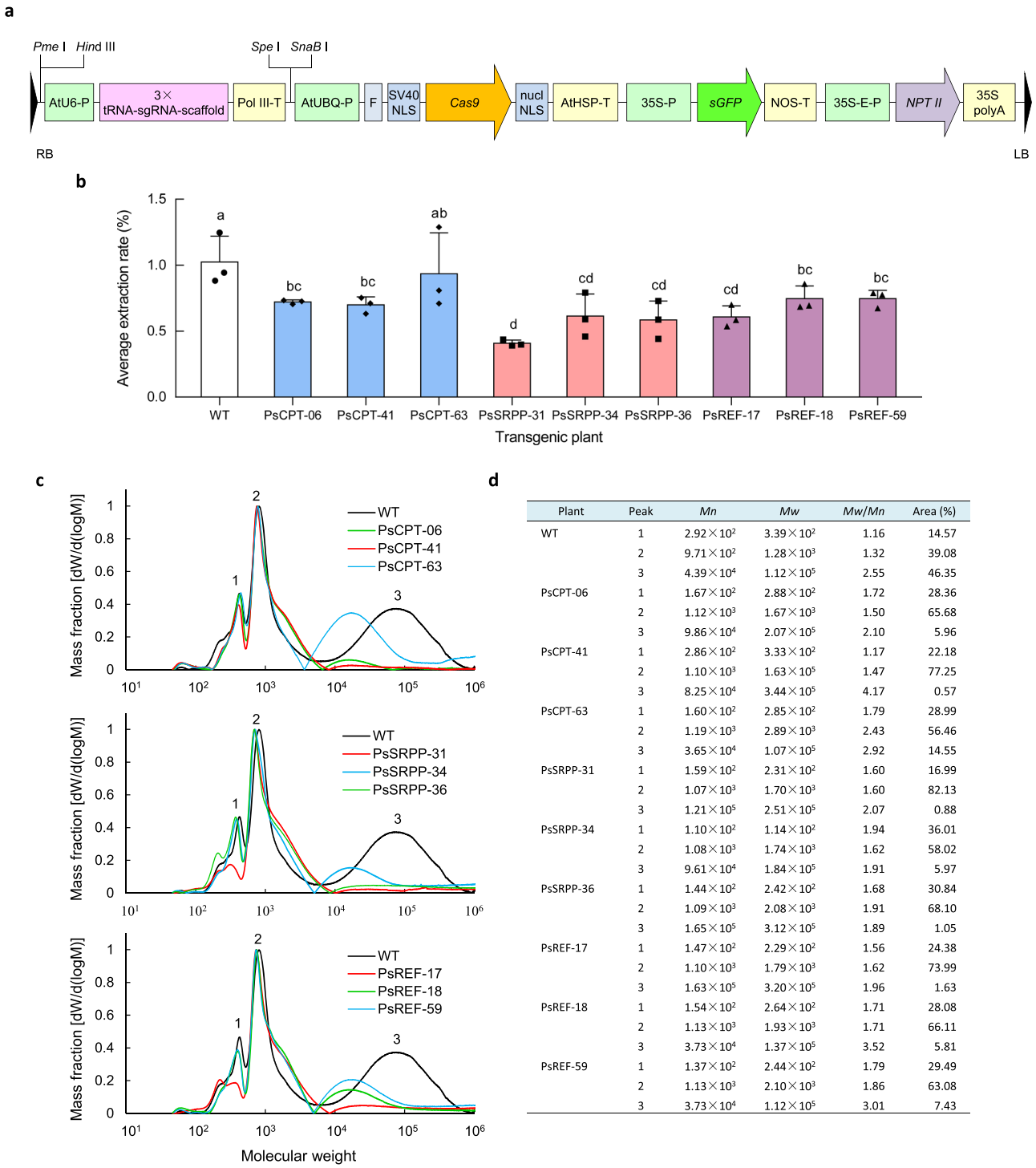

Plant	Peak	*Mn*	*Mw*	*Mw/Mn*	Area (%)
WT	1	2.92×10^{2}	3.39×10^{2}	1.16	14.57
	2	9.71×10^{2}	1.28×10^{3}	1.32	39.08
	3	4.39×10^{4}	1.12×10^{5}	2.55	46.35
PsCPT-06	1	1.67×10^{2}	2.88×10^{2}	1.72	28.36
	2	1.12×10^{3}	1.67×10^{3}	1.50	65.68
	3	9.86×10^{4}	2.07×10^{5}	2.10	5.96
PsCPT-41	1	2.86×10^{2}	3.33×10^{2}	1.17	22.18
	2	1.10×10^{3}	1.63×10^{3}	1.47	77.25
	3	8.25×10^{4}	3.44×10^{5}	4.17	0.57
PsCPT-63	1	1.60×10^{2}	2.85×10^{2}	1.79	28.99
	2	1.19×10^{3}	2.89×10^{3}	2.43	56.46
	3	3.65×10^{4}	1.07×10^{5}	2.92	14.55
PsSRPP-31	1	1.59×10^{2}	2.31×10^{2}	1.60	16.99
	2	1.07×10^{3}	1.70×10^{3}	1.60	82.13
	3	1.21×10^{5}	2.51×10^{5}	2.07	0.88
PsSRPP-34	1	1.10×10^{2}	1.14×10^{2}	1.94	36.01
	2	1.08×10^{3}	1.74×10^{3}	1.62	58.02
	3	9.61×10^{4}	1.84×10^{5}	1.91	5.97
PsSRPP-36	1	1.44×10^{2}	2.42×10^{2}	1.68	30.84
	2	1.09×10^{3}	2.08×10^{3}	1.91	68.10
	3	1.65×10^{5}	3.12×10^{5}	1.89	1.05
PsREF-17	1	1.47×10^{2}	2.29×10^{2}	1.56	24.38
	2	1.10×10^{3}	1.79×10^{3}	1.62	73.99
	3	1.63×10^{5}	3.20×10^{5}	1.96	1.63
PsREF-18	1	1.54×10^{2}	2.64×10^{2}	1.71	28.08
	2	1.13×10^{3}	1.93×10^{3}	1.71	66.11
	3	3.73×10^{4}	1.37×10^{5}	3.52	5.81
PsREF-59	1	1.37×10^{2}	2.44×10^{2}	1.79	29.49
	2	1.13×10^{3}	2.10×10^{3}	1.86	63.08
	3	3.73×10^{4}	1.12×10^{5}	3.01	7.43

Fig. 4 | Influence evaluation of PsCPT, PsSRPP and PsREF on rubber biosynthesis in *P. sepium* via CRISPR-Cas9 genome editing. a Schematic structure of the T-DNA region in the binary vector used for CRISPR-Cas9 genome editing of *PsCPT*, *PsSRPP* and *PsREF*; RB, right border; AtU6-P, *Arabidopsis thaliana* U6 promoter; 3×tRNA-sgRNA-scaffold, a tandemly arrayed three tRNA-sgRNA architecture containing tRNA-sgRNA1-scaffold-tRNA-sgRNA2-scaffold-tRNA-sgRNA3-scaffold of each *PsCPT*, *PsSRPP* or *PsREF* gene, respectively; Pol III-T, RNA polymerase III poly (T); AtUBQ-P, *A.thaliana* ubiquitin 10 promoter; F, 3×Flag-tag peptide; SV40 NLS, nuclear localization signal of simian virus 40 large T antigen; Cas9, endonuclease from the *Streptococcus pyogenes* type II CRISPR-Cas system; nucl NLS, bipartite nuclear localization signal from nucleoplasmin; AtHSP-T, *A.thaliana* heat shock protein 18.2 terminator; 35S-P, cauliflower mosaic virus (CaMV) 35S promoter; sGFP, synthetic green-fluorescent protein with S65T mutation; NOS-T, nopaline synthase terminator; 35S-E-P, CaMV 35S promoter with enhancer; NPT II, neomycin phosphotransferase; 35S poly A, CaMV 35S polyA terminator; LB, left border. **b** Three representative transgenic plants with mutations via CRISPR-Cas9 genome editing of each *PsCPT*, *PsSRPP* and *PsREF* gene, namely, transgenic PsCPT-06, PsCPT-41, and PsCPT-63; PsSRPP-31, PsSRPP-34, and PsSRPP-36; PsREF-17, PsREF-18, and PsREF-59, showed reduced total *cis*-polyisoprene contents to different degrees compared with that of the wild-type (non-transgenic negative, WT) control; Data represent mean ± standard deviation, $n = 3$; Different letters indicate significant differences at $p < 0.01$. **c**, **d** The transgenic plants with mutations exhibited the high-molecular-weight at approximately 10^4–10^6 (Peak3) shifted forwards and smaller or completely absent; These results indicated that mutagenesis of these three genes, *PsCPT*, *PsSRPP* and *PsREF*, can down-regulate the biosynthesis of *cis*-polyisoprenes in *P. sepium*.

accumulates in the laticifers both in the secondary phloem and pith as an end product. The rays may correlate with supplying the necessary network for *cis*-polyisoprene transport[39,42]. It has been reported that SRPPs generally have much higher rubber biosynthesis activity than Refs. 39,43–45. According to the BiFC assay, protein-protein interactions occur between PsCPT and PsSRPP, between PsSRPP and PsREF, and between PsCPT and PsREF. This result is analogous to reports in *H. brasiliensis*[46,47].

To further evaluate the comprehensive influences of the three genes encoding PsCPT, PsSRPP and PsREF on natural rubber biosynthesis, CRISPR-Cas9 genome editing was performed. Compared with that of the wild-type control, the total contents of the *cis*-polyisoprenes in the transgenic plants with deletion, substitution or insertion mutations were reduced to different degrees, and exhibited the high-molecular-weight peak at approximately 10^4–10^6 shifted forwards and smaller or completely absent. Our results demonstrated that *PsCPT*, *PsSRPP* and *PsREF* are the key genes that apparently play important roles in natural rubber biosynthesis and editing of these genes can significantly influence natural rubber content and molecular weight in *P. sepium*. As mentioned above, in chain extension during natural rubber biosynthesis, CPT has been identified from rubber-producing plants as a particle-bound rubber transferase responsible for the *cis*-1,4-polymerization of isoprene units from IPP onto the three kinds of allylic diphosphate primers, GPP, FPP and GGPP[4,48]. SRPP and REF are the two most abundant rubber particle proteins and are necessary for CPTs to incorporate IPP isoprene units into rubber molecules[4,43,45,49]. SRPP is speculated to generate mainly linear molecules with both high- and low-molecular-weight rubber chains, which are expected to be composed of active chain ends for chain elongation. On the other hand, REFs mostly compose branched molecules, which are expected to be derived from low-molecular-weight rubber chains via the aggregation of phospholipids on the surface of the rubber particle and play a termination role in the rubber elongation reaction[50]. Several previous reports have proved that CPTs, REFs and SRPPs are very crucial for rubber production, and down-regulation of these genes by RNA interference (RNAi) silencing or CRISPR-Cas9 knockout in *T. brevicorniculatum*, *T. kok-saghyz*, *Lactuca sativa*, often showed a significant reduction in latex content and natural rubber biosynthesis activity, but their molecular weight was not always changed[51–56].

P. sepium is a perennial shrub belonging to the family Asclepiadaceae and is widely distributed in temperate Asia, southern Europe, and tropical Africa[57,58]. *P. sepium* is excellent because of its high resistance to cold, drought, saline alkalis, and insects, and it can be planted in arid and semiarid areas[59,60]. Its suitable planting density is as high as 90,000/ha, and 135,000 kg/ha/year of branches and leaves can be harvested, according to our field experiments. Although the content of *cis*-polyisoprene is currently low, *P. sepium* is outstanding in its wide acclimatization, fast growth, and easy receptibility to genetic transformation[61] and may thus become an excellent experimental model plant for natural rubber biosynthesis research and an alternative source for natural rubber production. By identifying and overexpressing key genes that regulate polyisoprene biosynthesis, for example, the genes encoding CPT, SRPP, REF and their transcription factors or specific promoters[62] for polyisoprene chain elongation, the genes encoding GPP, FPP, GGPP synthases for the condensation of allylic diphosphate initiators, or even the genes for the precursor IPP supply in the mevalonic acid (MVA) and the 2-C-methyl-d-erythritol 4-phosphate (MEP) pathways, thereby increasing rubber content (yield) and quality (high-molecular-weight), transgenic *P. sepium* may become a promising rubber-producing plant that can be grown from tropical to temperate regions.

Methods

Polyisoprene extraction

To identify a plant that has potential for development as an alternative source for natural rubber production, three kinds of plants that produce latex, *P. sepium*, *A. venetum* and *C. chinense*, were selected. The rubber component polyisoprene was extracted from branches with leaves via Soxhlet extraction and solvent precipitation. Approximately 10 g of the branches with leaves from each plant were homogenized into powder in liquid nitrogen, and 1 g of powder from each sample was accurately weighed and pretreated with 30 mL of 10% sodium hydroxide in a boiling water bath for 3 h for degradation of the cuticle or fibres in the cell wall. The sludge was rinsed several times with deionized water until the effluent became neutral (usually five times) and then oven-dried at 40 °C before being transferred to a 250 mL Soxhlet apparatus. The sludge was treated with 100 mL of ethanol for 6 h to separate alcohol-soluble small molecule materials such as chlorophyll or pigments in advance. After oven drying at 40 °C, 100 mL of chloroform ($CHCl_3$; Meridian Medical Technologies, USA) was added to extract the polyisoprene in an 80 °C water bath for 6 h. The solvent was then collected and concentrated under vacuum in a rotator evaporator. The polyisoprene content of each sample was determined (% *w*/*w*) by weighing the residue obtained from chloroform extraction, which was repeated in triplicate[63].

GPC analysis

The molecular weight distribution of the polyisoprene extracted from the above 3 plants was determined via GPC (HLC-GPC8320, Tosoh, Japan) using two PL gel MIXED-B (10 μm, 7.5 × 300 mm) columns. The polyisoprene samples at 2 mg/mL in chloroform were prepared by filtering through a 0.45 μm microporous membrane. GPC was carried out at a column temperature of 40 °C, using chloroform as the eluent at a flow rate of 0.8 mL/min for 30 min. Twelve kinds of polystyrene (*Mw* 1.0×10^3–1.2×10^6, TSKgel Standard Polystyrene Oligomer Kit, Tosoh, Japan) at 1 mg/mL in chloroform were used as the calibration standard. A differential refractive detector (RI) was used to record the signal, and *Mn*, *Mw*, *Mw*/*Mn* of each sample were automatically calculated via the Eco-SEC Workstation provided by the GPC instrument.

NMR spectroscopy analysis

The polyisoprene extracted from *P. sepium*, a *cis*-1,4-polyisoprene standard from *H. brasiliensis* (average *Mw* 38000; Sigma-Aldrich, USA), and a pure *trans*-1,4-polyisoprene standard from *E. ulmoides* (a gift from Northwest A&F University, China), were dissolved in deuterated chloroform ($CDCl_3$, 99.8% Chloroform-*d* + 0.05% *v*/*v* tetramethylsilane; Cambridge Isotope Laboratories, USA) at a concentration of 50 mg/mL. ^{1}H-NMR and ^{13}C-NMR measurements were performed with a liquid NMR spectrometer (Avance NEO 700; Bruker, Germany) at 700 MHz and 298 K (25 °C) for 1 min and 4 h (corresponding to 16 scans and 7000 scans) respectively. Chemical shifts were reported with tetramethylsilane (TMS, 0.00 ppm) as an internal standard. The molecular structure was characterized by the chemical shift of the absorption peak in the NMR spectrum data via MestReNova software (Mestrelab Research SL, Spain).

Stem cryosection preparation

P. sepium stems approximately 10 mm in diameter were cut into 5-10 cm pieces and immediately fixed in 4% (*w*/*v*) freshly prepared paraformaldehyde (Macklin, China) in phosphate-buffered saline (PBS). The fixed stem was cut into 8 mm long pieces, rapidly embedded in Tissue-Tek O.C.T. compound (Sakura Finetechnical, Japan) and snap-frozen with liquid nitrogen. 60 μm-thick cryosections, including cross-sections and tangential sections, were prepared via a cryostat (CM-1950, Leica Microsystems, Germany) at −20 °C.

Histochemical staining

For histochemical staining, cryosections were mounted on glass slides and gently washed with PBS to remove the O.C.T. compound and were stained with 50 μg/mL Nile Red (Sigma-Aldrich, USA) in 50% ethanol for approximately 30 s to fluorescent stain the rubber components, such as *cis*-polyisoprenes and lipid bodies, followed by counterstaining with Calcofluor White stain (Sigma-Aldrich, USA) for approximately 30 min to stain the cell wall. After three washes in PBS, the sections were mounted in Vectashield mounting medium (Vector Laboratories, USA) and sealed with nail varnish as previously reported[39,40].

Primary antibody production

The three genes that encoded CPT, SRPP and REF were isolated from *P. sepium* according to genome and transcriptome sequencings, namely, *PsCPT* (AB082516), *PsSRPP* (PQ130390) and *PsREF* (PQ130391). The corresponding antigenic peptides MEKRSDQTSILENLC, CTDPADQPQMTEQEK and CMAASMATMKKESDG were synthesized and conjugated to keyhole limpet haemocyanin (KLH). A total of 400 μg of the synthetic peptides were used to immune New Zealand rabbits, which were boosted with 200 μg four times at 2-week intervals according to the company's standard protocol (Beijing Protein Innovation, China). Blood serum was collected from the carotid artery of the rabbit, and the titres of the antisera were over 1:25600, as determined via indirect enzyme-linked immunosorbent assay (ELISA). The specificity of each primary antibody against the proteins extracted from *P. sepium* was confirmed by Western blotting, and Alexa Fluor 555-labelled Donkey Anti-Rabbit IgG (Abcam, UK) was used as the secondary antibody.

Immunostaining

The immunostaining was modified from a previously reported method[33,39]. The cryosections were washed with PBS three times. The proteins in the sections were fixed with 4% paraformaldehyde in PBS for 30 min at room temperature, washed with PBS three times, blocked with 10% horse serum (Beijing Solarbio Science & Technology, China) in PBS for 30 min and then washed three times. The sections were subsequently reacted with 50 μL of each rabbit primary antibody diluted 1:100 in PBS, containing 10% horse serum and 0.1% Triton X-100 (Beijing Solarbio Science & Technology, China), and incubated overnight at 4 °C, protected from light. After being washed with PBS three times, the sections were incubated with 50 μL of the secondary antibody, Alexa Fluor 555-labelled Donkey Anti-Rabbit IgG diluted 1:200 for 2 h at room temperature. The sections were washed with PBS three times and further stained with Calcofluor White stain and mounted in mounting medium as described above.

SCLSM analysis

SCLSM analysis of the stained sections was performed at 25 °C via a spectral confocal laser scanning microscope system equipped with HC PL APO 10×, 20×, 40× lenses and Las X 4.4.0 software (Stellaris 5 DMi8, Leica Microsystems, Germany). The fluorescence was excited via the 405 nm line of a blue solid laser, and the 520 nm and 555 nm lines of a pulsed white laser, in all cases with laser power set to 2.0-10.0%. The emission spectra in the ranges of 410-560 nm, 525–675 nm, and 560–610 nm with 5 nm bandwidths were recorded for the detection of the cell wall stained with Calcofluor White stain, *cis*-polyisoprene stained with Nile Red and the secondary antibody stained with Alexa Fluor 555, respectively. Fresh latex of *P. sepium* tissue and the *cis*-1,4-polyisoprene standard from *H. brasiliensis* stained with Nile Red were used as reference samples. The ROIs fluorescence spectra from each of the 30 locations in the cell walls, *cis*-polyisoprenes and lipid bodies were measured and averaged from three successive scans to improve the signal-to-noise ratio. Image processing, including spectral unmixing, was performed via Las X 4.4.0 software.

BiFC assay

The full-length coding sequence (CDS) without the termination codon of each gene, *PsCPT*, *PsSRPP* and *PsREF*, was synthesized and constructed into binary vectors pSPYNE with N-terminal (1-155 amino acids + termination codon) of yellow fluorescent protein (YFP) and pSPYCE with C-terminal (156-239 amino acids + termination codon) of YFP for the BiFC assay[64]. The resultant vectors, pSPYNE-PsSRPP, pSPYNE-PsREF, pSPYCE-PsCPT, and pSPYCE-PsREF, were introduced into *Agrobacterium tumefaciens* strain EHA105 respectively, and were used for transient expression in tobacco according to the protocol described. The *Agrobacterium* harbouring pSPYCE-PsCPT and pSPYNE-PsSRPP, pSPYCE-PsCPT and pSPYNE-PsREF, pSPYCE-PsREF and pSPYNE-PsSRPP were suspended in infiltration buffer containing 10 mM 4-morpholineethanesulfonic acid (MES), 10 mM $MgCl_2$, and 200 mM acetosyringone, pH 5.7, to an optical density (OD_{600}) of 0.8 and then coinfiltrated into the abaxial side of *Nicotiana benthamiana* leaves. 48 h after infiltration, epidermal cell layers of the leaves were assayed for YFP fluorescence at an excitation wavelength of 514 nm.

CRISPR-Cas9 vector construction

Three different sgRNA (small guide RNA) target sites (N20) followed by NGG (the protospacer-adjacent motif, PAM) of each gene, *PsCPT*, *PsSRPP* and *PsREF*, were predicted and selected via CRISPR direct (http://crispr.dbcls.jp) (Supplementary Table 1). Each sgRNA target site was separated by a 77-bp-long pre-$tRNA^{Gly}$ sequence[65]. The three tandemly arrayed tRNA-sgRNA architectures of each gene were synthesized and constructed into a binary CRISPR-Cas9 vector, referred to as p*PsCPT*-3×sgRNA-Cas9, p*PsSRPP*-3×sgRNA-Cas9, and p*PsREF*-3×sgRNA-Cas9 (Fig. 4a). The resultant vectors were introduced into *A. tumefaciens* strain EHA105.

Gene transformation

Agrobacterium-mediated transformation and transgenic plant analysis were performed according to our previous reports[61]. Briefly, the stem segments of *P. sepium* were inoculated with *A. tumefaciens* strain EHA105 harbouring the three vectors. Through callus selection, adventitious shoot and root induction, the regenerated kanamycin-resistant plantlets were confirmed via PCR analysis to investigate the presence of the transgenes, using *Cas9*, *sGFP* and *NPT II* gene primers (Supplementary Table 2).

Transgenic plant analysis

Genomic DNA was isolated from the PCR-positive (PCR+) plantlets to screen for mutants by bidirectional sequencing spanning all the sgRNA target sites, using primer pairs (Supplementary Table 3) for each target gene, *PsCPT*, *PsSRPP* and *PsREF*. The plantlets containing mutations in the target genes were transplanted to a greenhouse for further growth for one year. Polyisoprene extraction and GPC analysis of the mutagenesis plants were performed as described above[63].

Statistics and reproducibility

In polyisoprene extractions from the three kinds of plants, *P. sepium*, *A. venetum* and *C. chinense*, and from the transgenic plants via CRISPR-Cas9 genome editing of *PsCPT*, *PsSRPP* and *PsREF*, all were repeated in triplicate ($n = 3$). Their one-way analysis of variance (ANOVA) and least significant difference (LSD) was calculated via Statistica software (StatSoft GmbH, Germany). The Dot-plots were generated using GraphPad Prism software (GraphPad Software, USA) and the statistical details were described in the figure legends.

Reporting summary

Further information on research design is available in the Nature Portfolio Reporting Summary linked to this article.

Data availability

Gene sequences of *PsCPT* (AB082516), *PsSRPP* (PQ130390) and *PsREF* (PQ130391) have been submitted to the National Center for Biotechnology Information (NCBI) database. All the data supporting the findings of this study are found within the manuscript and its supplementary data, and are available from the corresponding author upon request. The data used for generating graphs are shown in Supplementary Data 1.xlsx.

Received: 21 September 2024; Accepted: 13 February 2025;
Published online: 05 March 2025

References

1. Archer, B. L. & Audley, B. G. New aspects of rubber biosynthesis. *Bot. J. Linn. Soc.* **94**, 181–196 (1987).
2. Paterson-Jones, J. C., Gilliland, M. G. & van Staden, J. The biosynthesis of natural rubber. *J. Plant Physiol.* **136**, 257–263 (1990).

3. Men, X., Wang, F., Chen, G. Q., Zhang, H. B. & Xian, M. Biosynthesis of natural rubber: current state and perspectives. *Int. J. Mol. Sci.* **20**, 50 (2019).
4. Yamashita, S. & Takahashi, S. Molecular mechanisms of natural rubber biosynthesis. *Annu. Rev. Biochem.* **89**, 821–851 (2020).
5. Cornish, K. Similarities and differences in rubber biochemistry among plant species. *Phytochemistry* **57**, 1123–1134 (2001).
6. van Beilen, J. B. & Poirier, Y. Establishment of new crops for the production of natural rubber. *Trends Biotechnol.* **25**, 522–528 (2007).
7. Cherian, S., Ryu, S. B. & Cornish, K. Natural rubber biosynthesis in plants, the rubber transferase complex, and metabolic engineering progress and prospects. *Plant Biotechnol. J.* **17**, 2041–2061 (2019).
8. Cruz-Morales, J. A. et al. Synthetic polyisoprene rubber as a mimic of natural rubber: Recent advances on synthesis, nanocomposites, and applications. *Polymers* **15**, 4074 (2023).
9. Backhaus, R. A. Rubber formation in plants-a mini-review. *Isr. J. Bot.* **34**, 283–293 (1985).
10. Mooibroek, H. & Cornish, K. Alternative sources of natural rubber. *Appl. Microbiol. Biotechnol.* **53**, 355–365 (2000).
11. Tan, Y. C., Cao, J., Tang, C. R. & Liu, K. Y. Advances in genome sequencing and natural rubber biosynthesis in rubber-producing plants. *Curr. Issues Mol. Biol.* **45**, 9342–9353 (2023).
12. Chen, R., Harada, Y., Bamba, T., Nakazawa, Y. & Gyokusen, K. Overexpression of an isopentenyl diphosphate isomerase gene to enhance *trans*-polyisoprene production in *Eucommia ulmoides* Oliver. *BMC Biotechnol.* **12**, 78 (2012).
13. Ali, M. F., Akber, M. A., Smith, C. & Aziz, A. A. The dynamics of rubber production in Malaysia: Potential impacts, challenges and proposed interventions. *Policy Econ.* **127**, 102449 (2021).
14. Backhaus, R. A. & Nakayama, F. S. Variation in the molecular weight distribution of rubber from cultivated guayule. *Rubber Chem. Technol.* **61**, 78–85 (1988).
15. van Beilen, J. B. & Poirier, Y. Guayule and Russian dandelion as alternative sources of natural rubber. *Crit. Rev. Biotechnol.* **27**, 217–231 (2007).
16. Yang, N., Yang, D. D., Yu, X. C. & Xu, C. Multi-omics-driven development of alternative crops for natural rubber production. *J. Integr. Agric.* **22**, 959–971 (2023).
17. McFadyen, R. C. Biological control against parthenium weed in Australia. *Crop Prot.* **11**, 400–407 (1992).
18. Peng, T. X. et al. Introduction and trial planting of guayule. *Chin. J. Tropical Agric.* **27**, 1–11 (2007).
19. Lin, T. et al. Genome analysis of *Taraxacum kok-saghyz* Rodin provides new insights into rubber biosynthesis. *Natl. Sci. Rev.* **5**, 78–87 (2018).
20. Xie, Q. L. et al. Transcriptomics and proteomics profiles of *Taraxacum kok-saghyz* roots revealed different gene and protein members play different roles for natural rubber biosynthesis. *Ind. Crops Prod.* **181**, 114776 (2022).
21. Kuluev, B. et al. Molecular genetic research and genetic engineering of *Taraxacum kok-saghyz* L.E. Rodin. *Plants* **12**, 1621 (2023).
22. Tangpakdee, J., Tanaka, Y., Wititsuwannakul, R. & Chareonthiphakorn, N. Possible mechanisms controlling molecular weight of rubbers in *Hevea brasiliensis*. *Phytochemistry* **42**, 353–355 (1996).
23. Tanaka, Y., Sato, H. & Kageyu, A. Structural characterization of polyprenols by ^{13}C-n.m.r. spectroscopy: Signal assignments of polyprenol homologues. *Polymer* **23**, 1087–1090 (1982).
24. Tanaka, Y. Structure and biosynthesis mechanism of natural polyisoprene. *Prog. Polym. Sci.* **14**, 339–371 (1989).
25. Takeno, S. et al. High-throughput and highly sensitive analysis method for polyisoprene in plants by pyrolysis-gas chromatography/mass spectrometry. *Biosci. Biotechnol. Biochem.* **74**, 13–17 (2010).
26. Tanaka, Y., Sato, H. & Kagayi, A. Structure and biosynthesis mechanism of natural *cis*-polyisoprene from goldenrod. *Rubber Chem. Technol.* **56**, 299–303 (1982).
27. Tangpakdee, J. et al. Structure and biosynthesis of *trans*-polyisoprene from *Eucommia ulmoides*. *Phytochemistry* **45**, 75–80 (1997).
28. Tanaka, Y. & Hirasawa, H. Sequence analysis of polyprenols by 500 MHz ^{1}H-NMR spectroscopy. *Chem. Phys. Lipids* **51**, 183–189 (1989).
29. Thuong, N. T., Kosugi, K., Kawahara, S. & Nghia, P. T. Structural characterization of rubber from *Lactarius volemus* through 2D-NMR spectroscopy. *KGK RubberPoint* **68**, 26–32 (2015).
30. Tanaka, Y. & Tarachiwin, L. Recent advances in structural characterization of natural rubber. *Rubber Chem. Technol.* **82**, 283–314 (2009).
31. Jin, L. H. The analysis of branch and terminal group in natural rubber molecular chain. (Hainan University, 2017) (in Chinese with English abstract).
32. Wei, Y. C. Analysis and characterization of molecular structure of natural rubber. (Hainan University, 2020) (in Chinese with English abstract).
33. Kajiura, H., Suzuki, N., Mouri, H., Watanabe, N. & Nakazawa, Y. Elucidation of rubber biosynthesis and accumulation in the rubber producing shrub, guayule (*Parthenium argentatum* Gray). *Planta* **247**, 513–526 (2018).
34. Ahrends, A. et al. Current trends of rubber plantation expansion may threaten biodiversity and livelihoods. *Glob. Environ. Chang.* **34**, 48–58 (2015).
35. Schmidt, T. et al. Characterization of rubber particles and rubber chain elongation in *Taraxacum koksaghyz*. *BMC Biochem.* **11**, 11 (2010).
36. Cornish, K. The separate roles of plant *cis*- and *trans*-prenyl transferases in *cis*-4-polyisoprene biosynthesis. *Eur. J. Biochem.* **218**, 267–271 (1993).
37. Tanaka, Y., Kawahara, S., Eng, A. H., Takei, A. & Ohya, N. Structure of *cis*-polyisoprene from *Lactarius* mushroom. *Acta Biochim. Pol.* **41**, 303–309 (1994).
38. Yu T., Huang B. C., Yao W. & Ding H. D. Research and development of 3,4-polyisoprene rubber. *China Synth. Rubb. Ind*. **27**, 122–126 (2004) (in Chinese with English abstract).
39. Sando, T. et al. Histochemical study of detailed laticifer structure and rubber biosynthesis-related protein localization in *Hevea brasiliensis* using spectral confocal laser scanning microscopy. *Planta* **230**, 215–225 (2009).
40. Nakazawa, Y. et al. Histochemical study of trans polyisoprene accumulation by spectral confocal laser scanning microscopy and a specific dye showing fluorescence solvatochromism in the rubber producing plant, *Eucommia ulmoides* Oliver. *Planta* **238**, 549–560 (2013).
41. Gilliland, M. G. & van Staden, J. Detection of rubber in guayule (*Parthenium argentatum* Gray) at the ultrastructural level. *Z. Pflanzenphysiol.* **110**, 285–291 (1983).
42. Hebant, C. & Fay, E. Functional organization of the bark of *Hevea brasiliensis* (rubber tree): a structural and histoenzymological study. *Z. Pflanzenphysiol.* **97**, 391–398 (1980).
43. Oh, S. K. et al. Isolation, characterization, and functional analysis of a novel cDNA clone encoding a small rubber particle protein from *Hevea brasiliensis*. *J. Biol. Chem.* **274**, 17132–17138 (1999).
44. Ohya, N., Tanaka, Y., Wititsuwannakul, R. & Koyama, T. Activity of rubber transferase and rubber particle size in *Hevea* latex. *J. Rubber Res.* **3**, 214–221 (2000).
45. Xiang, Q. L. et al. Proteome analysis of the large and the small rubber particles of *Hevea brasiliensis* using 2D-DIGE. *Plant Physiol. Biochem.* **60**, 207–213 (2012).
46. Yamashita, S. et al. Identification and reconstitution of the rubber biosynthetic machinery on rubber particles from *Hevea brasiliensis*. *eLife* **5**, e19022 (2016).
47. Brown, D. et al. Subcellular localization and interactions among rubber particle proteins from *Hevea brasiliensis*. *J. Exp. Bot.* **68**, 5045–5055 (2017).

48. Asawatreratanakul, K. et al. Molecular cloning, expression and characterization of cDNA encoding *cis*-prenyltransferases from *Hevea brasiliensis*. *Eur. J. Biochem.* **270**, 4671–4680 (2003).
49. Dennis, M. S. & Light, D. R. Rubber elongation factor from *Hevea brasiliensis*. *J. Biol. Chem.* **264**, 18608–18617 (1989).
50. Tarachiwin, L., Sakdapipanich, J. T. & Tanaka, Y. Relationship between particle size and molecular weight of rubber from *Hevea brasiliensis*. *Rubber Chem. Technol.* **78**, 694–704 (2005).
51. Collins-Silva, J. et al. Altered levels of the *Taraxacum kok-saghyz* (Russian dandelion) small rubber particle protein, TkSRPP3, result in qualitative and quantitative changes in rubber metabolism. *Phytochemistry* **79**, 46–56 (2012).
52. Hillebrand, A. et al. Down-regulation of small rubber particle protein expression affects integrity of rubber particles and rubber content in *Taraxacum brevicorniculatum*. *PLoS One* **7**, e41874 (2012).
53. Post, J. J. et al. Laticifer-specific *cis*-prenyltransferase silencing affects the rubber, triterpene, and inulin content of *Taraxacum brevicorniculatum*. *Plant Physiol.* **158**, 1406–1417 (2012).
54. Laibach, N., Hillebrand, A., Twyman, R. M., Prüfer, D. & Gronover, C. S. Identification of a *Taraxacum brevicorniculatum* rubber elongation factor protein that is localized on rubber particles and promotes rubber biosynthesis. *Plant J.* **82**, 609–620 (2015).
55. Qu, Y. et al. A lettuce (*Lactuca sativa*) homolog of human Nogo-B receptor interacts with *cis*-prenyltransferase and is necessary for natural rubber biosynthesis. *J. Biol. Chem.* **290**, 1898–1914 (2015).
56. Kwon, M. et al. New insights into natural rubber biosynthesis from rubber-deficient lettuce mutants expressing goldenrod or guayule *cis*-prenyltransferase. *N. Phytol.* **239**, 1098–1111 (2023).
57. Yu, B., Ma, Y. M., Kong, Y. & Shi, Q. H. A study on chemical constituents of the stem of *Periploca sepium*. *Northwest For. Univ*. **20**, 145–146 (2005) (in Chinese with English abstract).
58. Ma, Y. M., Wang, P., Chen, L. & Feng, C. L. Chemical composition of the leaves of periploca sepium. *Chem. Nat. Compd.* **46**, 464–465 (2010).
59. Wang, X., Xia, J. B. & Cao, X. B. Physiological and ecological characteristics of *Periploca sepium* Bunge under drought stress on shell sand in the yellow river delta of China. *Sci. Rep.* **10**, 9567 (2020).
60. Wang, X. et al. Photosynthetic and water-related physiological characteristics of *Periploca sepium* in response to changing soil water conditions in a shell sand habitat. *J. Res.* **34**, 453–467 (2023).
61. Chen, R., Gyokusen, M., Nakazawa, Y., Su, Y. Q. & Gyokusen, K. Establishment of an *Agrobacterium*-mediated transformation system for *Periploca sepium* Bunge. *Plant Biotechnol.* **27**, 173–181 (2010).
62. Cui, S., Chen, R. & Qu, L. Q. Cloning and characterization of the promoters of the key genes *CPT*, *SRPP* and *REF* involved in *Periploca sepium* rubber biosynthesis. *Chin. J. Biotechnol.* **39**, 2794–2805 (2023).
63. Zhang, J. et al. Establishment of a microtube extraction method for natural rubber basic ingredient polyisoprene analysis. *J. Northwest. Univ.* **38**, 223–228 (2023).
64. Walter, M. et al. Visualization of protein interactions in living plant cells using bimolecular fluorescence complementation. *Plant J.* **40**, 428–438 (2004).
65. Xie, K. B., Minkenberg, B. & Yang, Y. N. Boosting CRISPR/Cas9 multiplex editing capability with the endogenous tRNA-processing system. *Proc. Natl. Acad. Sci. USA* **112**, 3570–3575 (2015).

Acknowledgements

This study was supported by National Natural Science Foundation of China (31460062, 31960065) and Key Research and Development Program of Ningxia (2019BFG02011).

Author contributions

J.J.Y. and G.D.L performed the experiments, data analysis and wrote the paper; Y.R.A participated in the experiments; S.R.L and H.Z. provided technical assistance and analyzed the data; R.C. provided guidance, supervision, and revised the paper. All authors have discussed the results of the manuscript.

Competing interests

The authors declare no competing interests.

Additional information

Supplementary information The online version contains supplementary material available at https://doi.org/10.1038/s42003-025-07734-4.

Correspondence and requests for materials should be addressed to Ren Chen.

Peer review information *Communications Biology* thanks Hector Garcia and Moslem Bahmankar for their contribution to the peer review of this work. Primary Handling Editors: Dr. Leena Tripathi and Dr. Ophelia Bu.